Desalination and Water Treatment
www.deswater.com

51 (2013) 1954–1965
February

Taylor & Francis
Taylor & Francis Group

doi: 10.1080/19443994.2012.715167

Biosorption of Cu^{2+} in a packed bed column by almond shell: optimization of process variables

Mónica Calero de Hoces*, Gabriel Blázquez García, Alicia Ronda Gálvez, Ana Estefanía Álvarez, María Ángeles Martín-Lara

Department of Chemical Engineering, University of Granada, 18071 Granada, Spain
Tel. +34 958 243311; Fax: +34 958 248992; email: mcaleroh@ugr.es

Received 7 February 2012; Accepted 18 July 2012

ABSTRACT

This paper presents the ability of a low-cost biosorbent, almond shell, to remove Cu(II) ions from aqueous solution. Biosorption capacity of almond shell to removal Cu(II) was studied in a packed bed column. The effect of various parameters, flow rate, initial copper concentration, and mass of biosorbent, was analyzed. A 2^3 factorial experiment design was carried out to optimize some of the factors directly affecting the biosorption of copper onto almond shell. The results have shown that initial concentration of Cu(II) is the most influential factors in biosorption capacity, while the most important factors in total copper removal are the flow rate and mass of biosorbent. The biosorption capacity of almond shell presented a maximum when the operational conditions are: flow rate, 6 mL/min; initial copper concentration, 100 mg/L; and mass of almond shell, 5 g; while the parameters which give the maximum value of % removal of Cu(II) are: flow rate, 2 mL/min; initial copper concentration, 40 mg/L; and mass of biosorbent, 15 g. The experimental breakthrough curves obtained under optimum conditions were modeled using Bohart–Adams, Thomas, Yoon–Nelson, and dose–response models. The Bohart–Adams model was valid only in representing the initial part of the breakthrough curves. The dose–response model is acceptable to reproduce the breakthrough curves.

Keywords: Biosorption; Copper; Almond shell; Column; Optimization

1. Introduction

Contamination of aqueous environment by heavy metals has been a major cause of concern over the last few decades, because heavy metals are nonbiodegradable and tend to accumulate in living organisms, thus becoming concentrated throughout the food chain [1]. Among the heavy metals in wastewaters, copper is considered having a high priority due to their toxicity and high disposal rate [2,3]. Conventional technologies for the removal of heavy metals include chemical precipitation, ion exchange, adsorption, evaporation, and membrane separation. The application of such traditional treatment techniques, however, needs enormous cost and continuous input of chemicals, which becomes impracticable and uneconomical and causes further environment damage [4–6]. Hence, the search for easy, effective, economic, and eco-friendly technique is necessary for treatment of effluent/wastewater treatment. Biosorption has been demonstrated as a

*Corresponding author.

Presented at the International Conference on Desalination for the Environment, Clean Water and Energy, European Desalination Society, 23–26 April 2012, Barcelona, Spain

potential, efficient, and economical method for the removal of heavy metals in wastewaters [7]. Different types of biomaterials, biomass of micro-organism, and agricultural waste, have been used for the removal of heavy metals using biosorption process. The availability of an effective biosorbent at low cost is a key factor dictating its selection for a biosorption process. Almond is one of the important crops grown in Andalucía, and the almond shell an important agricultural waste. In this respect, the almond shell is a good biosorbent to removal contaminants substances from aqueous solutions [8,9].

There are a lot of studies about removal heavy metals using batch mode of sorption experiments [10–13]. However, from an industrial point of view, the continuous biosorption in a packed bed column is often desired. There are a lot of factors (pH, temperature, flow rate, initial concentration of metal, and mass of biosorbent) influencing the biosorption process. The present study shows the effect of some them (flow rate, initial concentration of metal, and bed height) on the biosorption of Cu^{2+} onto almond shell.

Experimental design is an excellent tool for studying the individual and interaction effects or all parameters simultaneously [14,15]. The analysis in which the evaluation of more than one factor can be done is called full factorial analysis [16]. In full factorial multivariate experiment, all main factors and their interactions are compared with one another [17].

The objective of this work was: (1) to study the biosorption capacity of almond shell to removal of Cu (II) in a packed bed column, as well as to study the effect of different parameter in the biosorption process, (2) to optimize the process by factorial design, choosing the parameters which provide the best results in biosorption capacity and in the total Cu(II) removal, and (3) to model the breakthrough curves in the optimum conditions obtained in the factorial design.

Here, two-levels, three-factors (2^3) full factorial design (FFD) model was used [18]. The predicted result by the model was then compared with the experimental results.

For a proper design of an adsorption column, an accurate prediction for the breakthrough curve is needed. Therefore, some experimental results obtained (which optimizes the responses of the process) from the continuous system were fitted to four models: Adams–Bohart, Thomas, Yoon and Nelson, and dose–response models.

2. Materials and methods

2.1. Biosorbent: almond shell

Spain is the second mundial producer of almond, with 75,000 t/year. In Andalucia, Granada is one of the main places of production, with 5,900 t/year. The almond shell is a subproduct from peeled almonds. The almond shell was provided by Carsan Biocombustibles S.L. factory from Granada (Spain). The solid was milled with an analytical mill (IKA MF-10) and <1.000 mm fraction was chosen for the copper biosorption tests.

2.2. Continuous system

Continuous flow sorption experiments were conducted in a glass column with an internal diameter of 1.5 cm and length to 23 cm. A known quantity of the biosorbent was packed in the column to yield the corresponding bed height of the biosorbent. This bed of the biosorbent was supported between two small layers of cotton wool to prevent the biosorbent from floating. To enable a uniform inlet flow of the solution into the column, glass beads of 5 mm diameter were placed into the column. The copper solution having the desired initial concentration was then pumped through the column at desired volumetric flow rate with the help of a peristaltic pump (Dinko model D21 V) in an up-flow mode at constant temperature (maintained at 25°C with a thermostatic bath). Samples were collected from the outlet of the column at a time interval of 10 min during an operation time of 260 min and were analyzed by a 3100 Perkin–Elmer atomic absorption spectrophotometer to obtain the copper concentration of samples.

The experimental breakthrough curves were obtained measuring metal concentration in effluent samples collected. When the volume of the fluid begins to flow through the column, the mass-transfer zone varies from 0% of the inlet concentration, corresponding to the solute-free biosorbent, to 100% of the inlet concentration, corresponding to the total saturation, [19]. From a practical point of view, in this study, the saturation time, t_s, is established when the concentration in the effluent is the 90% of the inlet concentration; and the service or breakthrough time, t_r, is established when the metal concentration in the effluent reaches a value between 1 and 2 mg/L. The breakthrough curve is usually expressed in terms of a normalized concentration defined as the ratio of the effluent metal concentration to the inlet metal concentration (C/C_i) vs. time or volume of the effluent.

Analysis of column data was obtained and evaluated with the help of following equations:

- Volume of the effluent:

$$V_{ef} = Q \cdot t_{total} \quad (1)$$

- Total mass of metal biosorbed (the area under the breakthrough curve):

$$q_{total} = \frac{Q}{1000} \int_{t=0}^{t=t_{total}} C_R \cdot dt \quad (2)$$

- Total amount of metal ions sent to the column:

$$m_{total} = \frac{C_i \cdot Q \cdot t_{total}}{1000} \quad (3)$$

- Total metal removal (% R):

$$\%R = \frac{q_{total}}{m_{total}} \cdot 100 \quad (4)$$

- The amount of metal biosorbed at equilibrium or biosorption capacity:

$$q_e = \frac{q_{total}}{w} \quad (5)$$

- The equilibrium metal concentration:

$$C_e = \frac{m_{total} - q_{total}}{V_{ef}} \cdot 1000 \quad (6)$$

where V_{ef} is the volume of the effluent (mL), t_{total} is the total flow time (min), Q is the volumetric flow rate (mL/min), q_{total} is the total mass of metal biosorbed (mg), C_R is the concentration of metal removal (mg/L), m_{total} is the total amount of metal ions sent to the column (mg), % R is the total metal removal (%), q_e is the amount of metal biosorbed at equilibrium or biosorption capacity (mg of sorbated metal/g of biosorbent), w is the mass of the biosorbent (g), and C_e is the equilibrium metal concentration (mg/L).

2.3. Statistical optimization

The factorial design describes which factor shows more impact and influence the variation of one factor on the other factors [20]. In this work, volumetric flow rate, initial Cu(II) concentration, and biosorbent dose were taken as independent variables while the other variables like the particle size (<1 mm), temperature (25˚C), and total flow time (260 min) were kept constants. Responses examined were the biosorption capacity and total Cu(II) removal. Two replicates of 2^3 FFD having eight experiments (with one replicate) were studied. The three factor and two levels for almond shell are shown in Table 1.

Table 1
Values and levels of operating parameters for almond shell

Factors	Levels	
	(−1)	(+1)
X_1: volumetric flow rate, mL/min	2	6
X_2: initial copper concentration, mg/L	40	100
X_3: mass of biosorbent, g	5	15

2.4. Modeling data

The development of a model that describes such a concentration-time profile is difficult in most cases, because the metal concentration in the liquid continuously changes and, therefore, the process does not operate at steady state. The fundamental equations for a fixed-bed column depend on the mechanism responsible for the process (mass transfer from the liquid to the surface of the solid, diffusion, and/or reaction on the surface of the solid) and include mass balances between the solid and fluid and for the sorbed solute, rate of the process, etc. The equations derived to model the system with theoretical rigor are differential in nature and usually require complex numerical methods to solve. Because of this, various simple mathematical models such as the Adams–Bohart, Thomas, Yoon and Nelson, and dose–response models have been developed to predict the dynamic behavior of the column and allow some kinetic coefficients to be estimated. However, they do not contain any mass-transfer consideration and, therefore, are less rigorous than other theoretical models.

These models are described below. To choose them, the conditions of application of each one of them and their use for the study of biosorption in a column have been considered by the majority of researchers [21–25].

2.4.1. Adams–Bohart model

Adams and Bohart [26] established the fundamental equation, which describes the relationship between C/C_i and t in a continuous system, and although it was originally applied to a gas–solid system, it has been extensively used to describe and quantify other types of systems. This model assumes that the sorption rate is proportional to the residual capacity of the solid and the concentration of the sorbed substance and is used to describe the initial part of the breakthrough curve. Its equation can be described as

$$\frac{C}{C_i} = \frac{e^{k_{AB} \cdot C_i \cdot t}}{e^{\frac{k_{AB} \cdot N_0 \cdot Z}{v}} - 1 + e\, k_{AB} \cdot C_i \cdot t} \quad (7)$$

where k_{AB} is the kinetic constant (L/mg min), N_0 is the maximum volumetric sorption capacity (mg/L), C is the solute concentration in the liquid phase in (mg/L), C_i is the inlet metal concentration (mg/L), v is the linear flow rate (cm/min), t is the time (min), and Z is the bed depth in the column (cm).

Because $e^{\frac{k_{AB} \cdot N_0 \cdot Z}{V}}$>>1 and this model is going to be applied to describe the initial part of the breakthrough curve ($C < 0.15C_i$), the Adams–Bohart model is reduced to the following simplified equation

$$\frac{C}{C_i} = e^{k_{AB} \cdot C_i} \cdot t - \frac{k_{AB} \cdot N_0 \cdot z}{v} \quad (8)$$

2.4.2. Thomas model

The Thomas model [27] is one of the most general and widely used to describe the behavior of the biosorption process in fixed-bed columns. Its main limitation is that its derivation is based on second-order kinetics and considers that sorption is not limited by the chemical reaction, but controlled by mass transfer at the interface. This discrepancy can lead to errors when this method is used to model biosorption processes in specific conditions [21]. This model can be described by the Eq. (9)

$$\frac{C}{C_i} = \frac{1}{1 + \mathrm{e}^{\left(\frac{k_{Th}}{Q}(q_o \cdot w - C_i \cdot V_{ef})\right)}} \quad (9)$$

where k_{Th} is the Thomas rate constant (mL/min mg) and q_0 is the maximum concentration of the solute in the solid phase (mg/g).

2.4.3. Yoon and Nelson model

Yoon and Nelson [28] developed a relatively simple model focused on the adsorption of vapors or gases in activated coal. This model assumes that the rate of decrease in the probability of adsorption for each adsorbate molecule is proportional to the probability of sorbate sorption and the probability of sorbate breakthrough on the biosorbent. The Yoon and Nelson model not only is less complex than other models but also does not require related data on the adsorbate characteristics, the type of adsorbent, or the physical properties of the bed. Eq. (10) represents this model

$$\frac{C_i}{C} = \frac{1}{1 + e^{k_{YN} \cdot (\tau - t)}} \quad (10)$$

where k_{YN} is the Yoon and Nelson's proportionality constant (min) and τ is the time required for removal 50% of the initial metal (min).

It should be indicated that the expression of the Yoon and Nelson model is mathematically analogous to the equation of the Thomas model.

2.4.4. Dose–response model

This model, which has been commonly used in pharmacology to describe different types of processes, is currently being applied to describe biosorption in the columns [29,30].

The general equation, which represents this model, is

$$Y = b_0 - \frac{b_0}{1 + \left(\frac{X}{b_2}\right)^{b_1}} \quad (11)$$

where X and Y represent the dose and response, respectively, in terms of the percentage of maximum possible response. The parameter b_0 is the expected response when saturation is reached, b_1 represents the slope of the function, and b_2 indicates the concentration at which half of the maximum response occurs.

When application of this equation is considered for the study of biosorption in the columns, Y would represent the relationship of concentrations, C/C_i, and X is the time or volume of the liquid that circulates through the column. Therefore, the parameter b_0 is equal to 1 because the maximum value of C/C_i is 1 when the time or volume tends to ∞. On the basis of these considerations, this equation can be rewritten as follows:

$$\frac{C}{C_i} = 1 - \frac{1}{1 + \left(\frac{V_{ef}}{b}\right)^{a}} \quad (12)$$

When the retention reached is 50%, this one can be rewritten as:

$$0.5 = 1 - \frac{1}{1 + \left(\frac{0.5 \cdot V_{ef}}{b}\right)^a} \tag{13}$$

and therefore,

$$\left(\frac{0.5 \cdot V_{ef}}{b}\right)^a = 1 \tag{14}$$

Because $b \neq 0$, $0.5V_{ef}/b = 1$ and $b = 0.5V_{ef}$.

In accordance with the Thomas model previously mentioned, it can be determined that $0.5V_{ef} = q_0 w / C_i$, and, therefore, the dose–response model would be represented by the equation

$$\frac{C}{C_i} = 1 - \frac{1}{1 + \left(\frac{C_i \cdot V_{ef}}{q_0 \cdot w}\right)^a} \tag{15}$$

where a is the constant of model.

This model has a relative importance, because it describes, usually very exactly the full breakthrough curve, but it is difficult to relate the empirical parameter "a" with the experimental conditions. Thus, it is very difficult its implementation to carry out a change of system scale [31].

3. Results and discussions

3.1. Biosorption of Cu(II)

3.1.1. Effect of feed flow rate

First, the effect of feed flow rate has been analyzed. For that, other parameters have been kept constant according previous studies performed in batch [32] and data from literature: initial concentration of Cu(II), 40 mg/L; pH 5; time of contact, 260 min; and mass of almond, 5 g (equivalent to 4.4 cm of high bed column). For all experiments, $t = 0$ has been assigned to the time in the exit of the column, with the objective that all them have the same referent point.

The breakthrough curves to three flow rates (2, 4, and 6 mL/min) have been illustrated in Fig. 1.

The removal of Cu increases while the flow rate decreases, reaching the saturation of the column only when the flow rate is 6 mL/min.

Also, the breakthrough time, t_r, (considering that it reaches when the concentration of effluent has a value between 1 and 2 mg/L) increases when the flow rate decreases. Thus, for a flow rate of 2 mL/min, the breakthrough time is higher than 50 min, while for a flow rate of 6 mL/min, the breakthrough time practically coincides with the initial time.

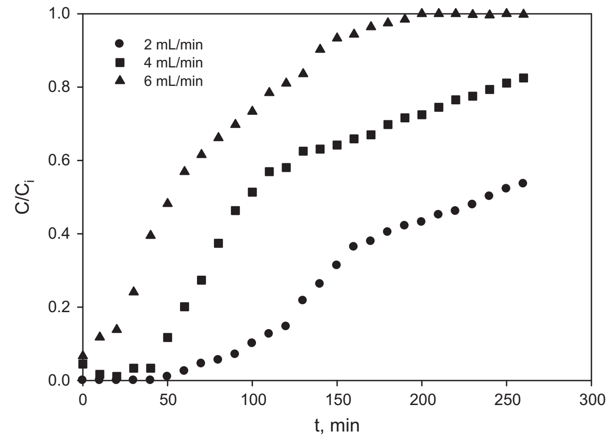

Fig. 1. The effect of feed flow rate on biosorption of Cu(II) onto almond shell ([Cu(II)] = 40 mg/L, m = 5 g, t = 260 min, and T = 298 K).

To verify and to compare these results, experiments have been performed changing the initial concentration of copper and keeping constant the other experimental parameters. In Fig. 2, the results are obtained when initial concentration of Cu(II) (100 mg/L) is represented.

It observed that, when initial concentration of copper is increased, results are similar to obtained initial concentration of 40 mg/L. However, as initial concentration increases, does not initially remove all copper present in the solution, and saturation of column is reached more quickly. These results are similar to report of other authors in packed bed column systems with different heavy metals and different biosorbents [33–35].

These results show that, from view point of operation of the column, the best results are obtained with

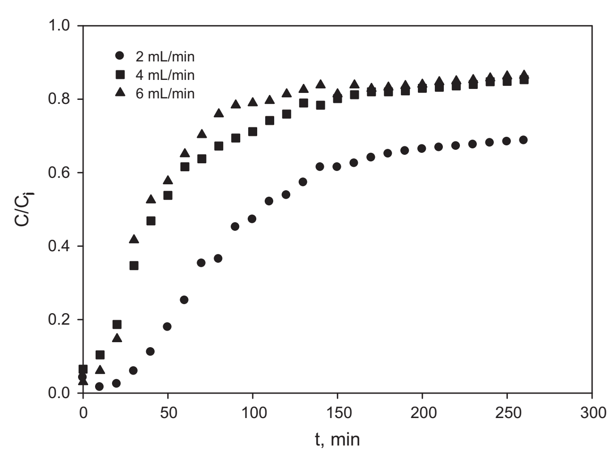

Fig. 2. The effect of feed flow rate on biosorption of Cu(II) onto almond shell ([Cu(II)] = 100 mg/L, m = 5 g, t = 260 min, and T = 298 K).

a flow rate of 2 mL/min, due to the higher breakthrough time and produced a higher removal of Cu(II).

3.1.2. Effect of bed height

The removal of metals in a packed bed column depends among other factors; the amount of biosorbent used (or bed height of column). Therefore, the effect of mass of biosorbent on biosorption of Cu(II) has been studied. For that, are performed experiments with two amounts of biosorbent, equivalents to two bed height, 5 g (4.4. cm) and 15 g (13.4 cm). According to previous results, flow rate of 2 mL/min and two initial concentrations of Cu(II), 40 and 100 mg/L, have been chosen. Results are showed in Figs. 3 and 4.

Figures show that, for two concentrations used, an increase in bed height increases the copper removal. As the bed height increases, Cu(II) had more time to contact with almond shell that resulted in higher removal efficiency of Cu(II) ions in column. So the higher bed column results in a decrease in the solute concentration in the effluent at the same time. The slope of breakthrough curve decreased with increasing bed height, which resulted in a broadened mass transfer zone. High uptake was observed at the highest bed height due to an increase in the surface area of biosorbent, which provided more binding sites for the sorption [36,37].

Observing the variation of the breakthrough time from Figs. 3 and 4, it verified that, t_r decreases significantly for a bed height of 4.4 cm (5 g of biosorbent). On the other hand, for these experimental conditions, the saturation of the column is not reached in any experiments performed to the operational time considered.

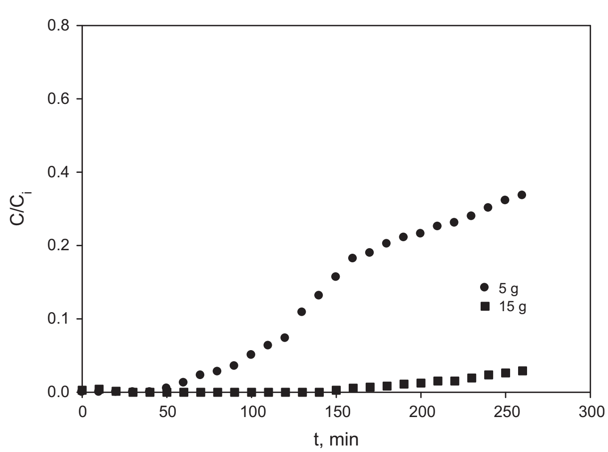

Fig. 3. The effect of mass of biosorbent on biosorption of Cu (II) onto almond shell([Cu(II)] = 40 mg/L, flow rate = 2 mL/min, t = 260 min, and T = 298 K).

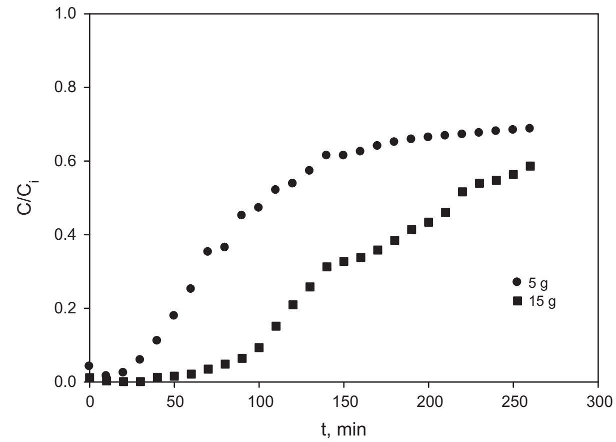

Fig. 4. The effect of mass of biosorbent on biosorption of Cu(II) onto almond shell ([Cu(II)] = 100 mg/L, flow rate = 2 mL/min, t = 260 min, and T = 298 K).

3.2. Statistical analysis

A two-level, three-factors FFD of response surface methodology was applied to predict the effect of volumetric flow rate, initial copper concentration, and biosorbent dose on the biosorption capacity and on the removal of Cu(II) in column system. The parameters were coded at two levels: −1 and +1. The results obtained were evaluated for the biosorption capacity and for the removal efficiency of Cu(II). The design matrix along with the experimental and predicted results is shown in Table 2.

The predicted responses for Cu(II) uptake (biosorption capacity and total Cu(II) removal) were obtained and are given as:

- Biosorption capacity (Eq. 16): $R^2 = 0.9829$, R^2 (adjusted) = 0.9715

$$q_e = 4.456 + 1.126 \cdot X_1 + 1.859 \cdot X_2 - 1.309 \cdot X_3 + 0.644 \cdot X_1 \cdot X_2 + 0.061 \cdot X_1 \cdot X_3 - 0.841 \cdot X_2 \cdot X_3$$

- Total Cu(II) removal (Eq. (17)): $R^2 = 0.9653$, R^2 (adjusted) = 0.9420

$$\% R = 60.923 - 15.1240 \cdot X_1 - 9.428 \cdot X_2 + 14.645 \cdot X_3 + 2.255 \cdot X_1 \cdot X_2 + 3.653 \cdot X_1 \cdot X_3 - 4.480 \cdot X_2 \cdot X_3$$

In these equations, q_e and % R are the predicted responses variables; X_1, X_2, and X_3 are independent variables in coded unit; and $X_1 \cdot X_2$, $X_1 \cdot X_3$, and $X_2 \cdot X_3$ are interactive terms.

The interaction effects are easily estimated and tested through the usual analysis of variance (ANOVA). ANOVA is a statistical method that

Table 2
FFD matrix for almond shell. Natural and coded values of parameters

Runs	Coded values			Natural values			Responses			
							Experimental		Predicted	
	X_1	X_2	X_3	Volumetric flow rate, mL/min	Initial Cu(II) concentration, mg/L	Mass of biosorbent, g	q_e, mg/g	% R	q_e, mg/g	% R
1	−1	−1	−1	2	40	5	3.00	76.73	3.400	72.258
2	+1	−1	−1	6	40	5	3.13	25.72	4.243	30.194
3	−1	+1	−1	2	100	5	6.40	53.37	5.999	57.852
4	+1	+1	−1	6	100	5	10.53	29.29	9.417	24.808
5	−1	−1	+1	2	40	15	1.23	98.72	0.829	103.202
6	+1	−1	+1	6	40	15	3.03	80.23	1.915	75.750
7	−1	+1	+1	2	100	15	2.69	75.35	3.091	70.876
8	+1	+1	+1	6	100	15	5.64	47.97	6.753	52.444

partitions the total variation into its component parts each of which is associated with a different source of variation [38]. This procedure performs a multifactor ANOVA for biosorption capacity (q_e) and for total copper removal (% R). It constructs various tests and graphs to determine which factors have a statistically significant effect on removal. It also tests for significant interactions amongst the factors, given sufficient data. The F-tests in the ANOVA table allows identifying the significant factors. The ANOVA results for Cu (II) are shown in Table 3. The sum of squares used to estimate factors effects, and Fisher's F-ratios and P-values are also shown in the table. From the ANOVA for q_e and % R (Type III sums of squares), it was observed that since five P-values are less than 0.05 (except corresponding of interaction between flow rate and mass of biosorbent and interaction between initial copper concentration and mass of biosorbent for q_e and % removal, respectively), these factors have a statistically significant effect on biosorption capacity at the 95.0% confidence level.

Graphs of the predicted response values vs. the experimental response values for q_e and % R are shown in Figs. 5 and 6, respectively. They help to detect a value, or group of values, that are not easily predicted by the model. These figures show that the

Table 3
ANOVA for q_e and for % of Cu(II) removal. ANOVA table

Response	Source	Sum of squares	df	Mean square	F-ratio	P-value
q_e	X_1	20.295	1	20.295	58.83	0.0000
	X_2	55.279	1	55.279	160.24	0.0000
	X_3	27.405	1	27.405	79.44	0.0000
	$X_1 \times X_2$	6.631	1	6.631	19.22	0.0018
	$X_1 \times X_3$	0.060	1	0.060	0.17	0.6864
	$X_2 \times X_3$	11.323	1	11.323	32.82	0.0003
	Residual	3.105	9	0.345		
	Total (corr.)	124.098	15			
% R	X_1	3,657.830	1	3,657.830	99.86	0.0000
	X_2	1,422.040	1	1,422.040	38.82	0.0002
	X_3	3,432.620	1	3,432.620	93.69	0.0000
	$X_1 \times X_2$	81.360	1	81.360	2.22	0.1703
	$X_1 \times X_3$	213.452	1	213.452	5.83	0.0390
	$X_2 \times X_3$	321.126	1	321.126	8.77	0.0159
	Residual	329.651	9	36.628		
	Total (corr.)	9,457.08	15			

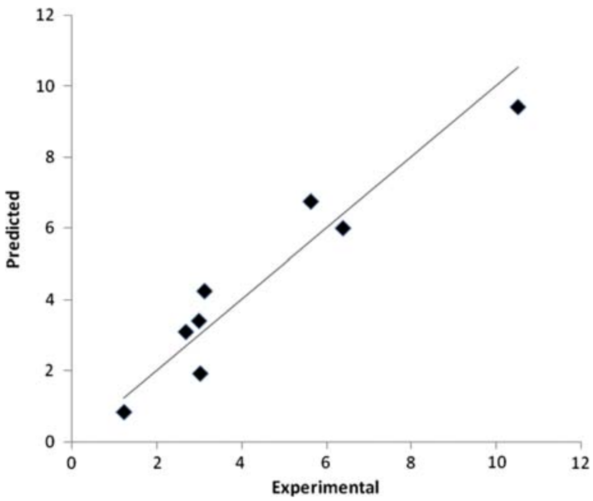

Fig. 5. Scatter graph of the predicted response values vs. experimental response values for the biosorption capacity of Cu(II) onto almond shell.

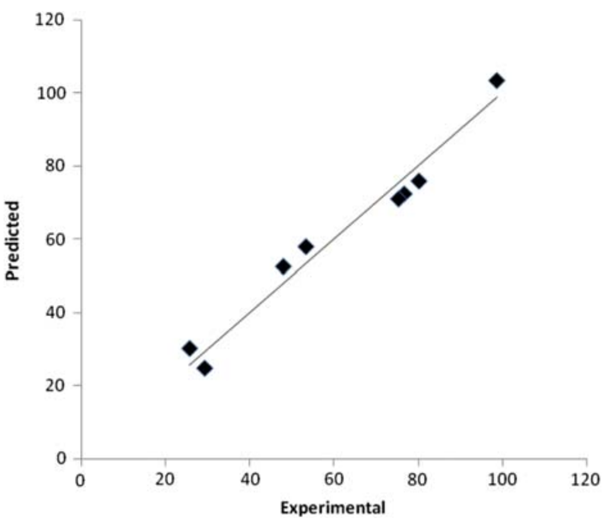

Fig. 6. Scatter graph of the predicted response values vs. experimental response values for total Cu(II) removal (% *R*) onto almond shell.

develop models were adequate because the residuals for the prediction of each response are in minimum.

To evaluate the statistical significance of the factors and their interaction on the response was analyzed through Pareto diagram. This diagram represents all factors involved in the process in order of importance. Fig. 7 shows that initial concentration of Cu(II) which is the most influential factors in biosorption capacity, while the most important factor in total copper removal (Fig. 8) are the flow rate and mass of biosorbent as reported from other authors [18].

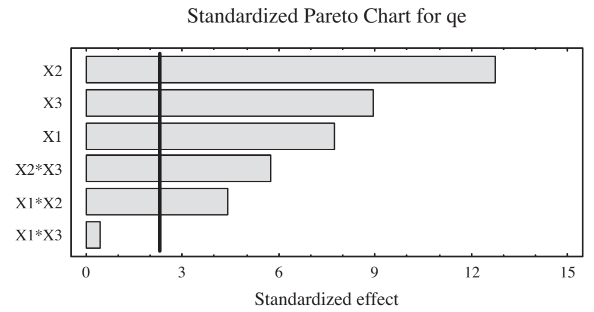

Fig. 7. The Pareto plot for the biosorption capacity.

From the statistical optimization, it observed that the optimum values to maximize the biosorption capacity (10.53 mg/g) for flow rate, initial Cu(II) concentration, and mass of almond shell were estimated to be 6 mL/min, 100 mg/L and 5 g, respectively; while to maximize the % of copper removal (98.72%) was estimated to be 2 mL/min, 40 mg/L, and 15 g, respectively, for each factors.

3.3. Breakthrough curves

3.3.1. Determination of kinetic parameters

To obtain the breakthrough curve to biosorption of Cu(II) on almond shell, experiments have been performed with optimum conditions of the packed bed column. In this sense, the parameters have been chosen which give the maximum value of % removal of Cu(II) in a column (flow rate = 2 mL/min, C_i = 40 mg/L, and mass of biosorbent = 15 g (bed height = 13.4 cm)) and the maximum value of biosorption capacity (flow rate = 6 mL/min, C_i = 100 mg/L, and mass of biosorbent = 5 g (bed height = 4.4 cm)). Results have also been included that were obtained for the experimental conditions (flow rate = 6 mL/min, C_i = 100 mg/L, and mass of biosorbent = 15 g (bed height = 13.4 cm)) with the objective to include the effect of the bed height, keeping others experimental parameters constant. All

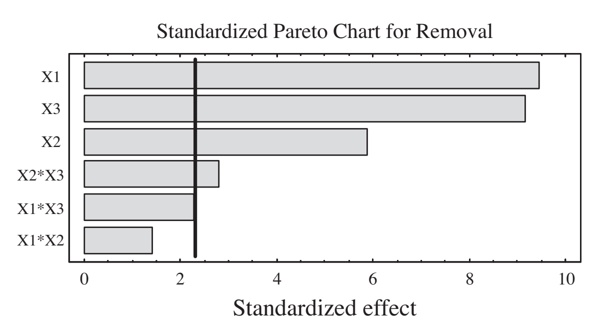

Fig. 8. The Pareto plot for the % of copper removal.

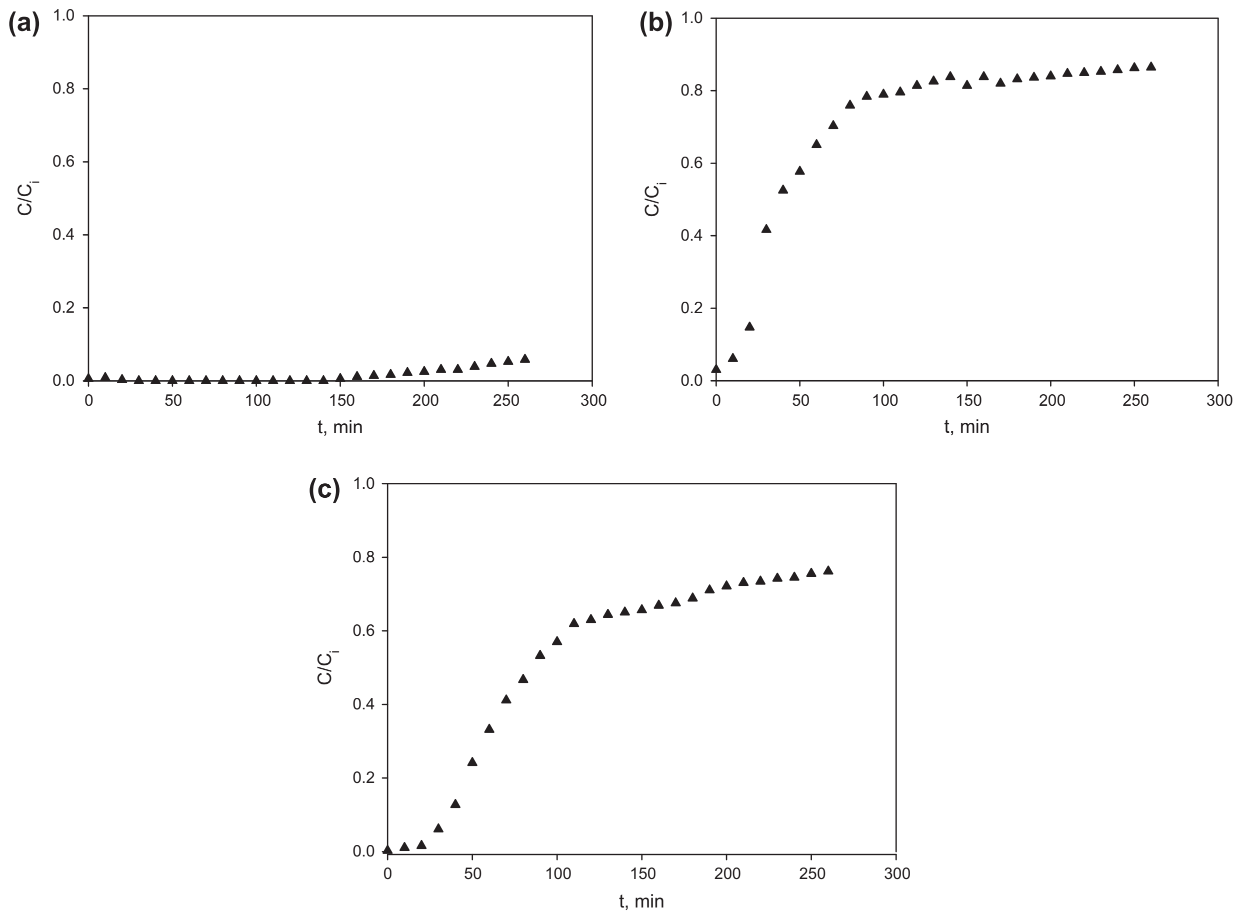

Fig. 9. Breakthrough curves for Cu(II) biosorption onto almond shell at pH = 5: (a) amount of almond shell = 15 g; flow rate = 2 mL/min; and C_i = 40 mg/L; (b) amount of almond shell = 5 g; flow rate = 6 mL/min; and C_i = 100 mg/L; and (c) amount of almond shell = 15 g; flow rate = 6 mL/min; and C_i = 100 mg/L.

experiments have been performed with a constant temperature 25°C, pH = 5, and contact time = 260 min. The saturation time, t_s, has been established when the C/C_i is higher than 0.9, as is usual in this studies. Results obtained are shown in Fig. 9(a)–(c).

From the experimental data of Fig. 9(a)–(c) were obtained the most significant parameters of the breakthrough curves according to Eqs. (1)–(6). These results are summarized in Table 4.

Comparing data from Table 4, in first test (Fig. 9 (a)), the value of % removal of Cu(II) is close to 100%, while the biosorption capacity is very low, 1.23 mg/g. However, in second test (Fig. 9(b)), the biosorption capacity is much higher, 10.53 mg/g, while the % removal is very low, 30% approximately. Increasing the bed height keeping conditions of second test (Fig. 9(c)), improves significantly % removal of copper, but decreases biosorption capacity practically to half of maximum value obtained. It is noted that a increasing in bed height keeping other experimental parameters has a negative effect in biosorption capacity and a positive effect in % removal of Cu(II).

Table 4
Parameters of the breakthrough curves for almond shell for different experimental conditions

	V_{ef}, mL	q_{total}, mg	m_{total}, mg	% R	q_e, mg/g	C_e, mg/L	t_r, min	t_s, min
Fig. 9a	520	18.48	18.72	98.72	1.23	0.47	200	–
Fig. 9b	1,560	52.65	179.77	29.29	10.53	81.49	–	260
Fig. 9c	1,560	84.57	176.28	47.97	5.64	58.78	10	–

From respective breakthrough time and saturation time it is observed that, for the first, there is a high difference with experimental conditions used: so, in first test it resulted in a breakthrough time of 200 min, compared with 10 min obtained in the last test, and this has not been obtained in second test. On the other hand, the saturation of the column only is achieved in second test (Fig. 9(b)).

3.3.2. Modeling of data

In the following sections, the experimental results from Fig. 9(b) and (c) ($Q = 6$ mL/min; $C_i = 100$ mg/L; and $z = 4.4$ and 13.4 cm, respectively) have been fitted to each of the models mentioned previously with the aim of describing the fixed-bed column behavior, determining the corresponding kinetic parameters. The experimental results were fitted to the models through nonlinear regressive analysis using the Marquardt algorithm. Below results obtained are discussed.

Adams–Bohart model. In accordance with numerous authors, the Adams–Bohart model is mainly used when the concentration in the effluent is lower than $0.15C_i$, (of initial part of breakthrough curve) [21,39,40]. The model parameters were obtained using nonlinear regression analysis according to Eq. (8), and the results are listed in Table 5.

Adams–Bohart model reproduces acceptably the initial part of the breakthrough curve in both cases studied. The volumetric biosorption capacity, N_0, decreases with increases bed height, equal that kinetic constant, k_{AB}, which also decreases with bed height, indicating that the biosorption process occurs more slowly. These results are similar to obtained by other authors [41–43].

Thomas model. The Thomas model is one of the most widely used methods to describe column biosorption data. According to Eq. (9) and nonlinear regression are obtained parameters model and adjusted values. They are shown in Table.

The Thomas model does not reproduce the breakthrough curves acceptably (see the r^2 values). Furthermore, comparing results (Table 5), it is observed that values of maximum concentration of the solute in the solid phase, q_0, are lower than experimental values (especially in first case). Results obtained by other authors with Thomas model are very different. So, Vázquez et al. [44] studying the optimization of biosorption of lead, copper, and zinc onto nut shell indicate that Thomas model does not reproduce acceptably the breakthrough curves, finding differences between experimental values of biosorption capacity and the values obtained by model. Han et al. [42] study the adsorption of copper in a packed bed

Table 5
Estimated parameter values for the Adams–Bohart, Thomas, Yoon–Nelson, and dose–response models for the biosorption process of Cu(II) onto almond shell

Adams–Bohart model						
Figure	Z, cm	k_{AB}, L/mg min	N_0, mg/L	r^2	$\sum[(C/C_i)_{exp} - (C/C_i)_{cal}]^2$	
Fig. 9(b)	4.4	8.56×10^{-4}	3461.2	0.998	0.0001	
Fig. 9(c)	13.4	4.69×10^{-4}	2285.6	0.973	0.0027	
Thomas model						
Figure	Z, cm	K_{Th}, mL/mg min	q_0, mg/g	r^2	$\sum[(C/C_i)_{exp} - (C/C_i)_{cal}]^2$	
Fig. 9(b)	4.4	0.191	7.399	0.782	0.352	
Fig. 9(c)	13.4	0.127	5.280	0.839	0.291	
Yoon–Nelson model						
Figure	Z, cm	K_{YN}, mL/mg min	τ_{cal}, min	τ_{exp}, min	r^2	$\sum[(C/C_i)_{exp} - (C/C_i)_{cal}]^2$
Fig. 9(b)	4.4	0.0220	53.5	45	0.782	0.352
Fig. 9(c)	13.4	0.0143	116.8	90	0.839	0.291
Dose–response model						
Figure	Z, cm	a	b	q_0, mg/g	r^2	$\sum[(C/C_i)_{exp} - (C/C_i)_{cal}]^2$
Fig. 9(b)	4.4	1.288	5.802	0.964	0.0583	1.288
Fig. 9(c)	13.4	1.472	4.404	0.970	0.0535	1.472

Table 6
Experimental and calculated values of total amount of copper retain in the column, q_{total}

	q_{total} (exp.), mg	q_{total} (calc.), mg
Fig. 9(b)	52.65	50.99
Fig. 9(c)	84.57	83.16

column using zeolites coated of iron oxide and they show that Thomas model reproduces well the breakthrough curves, obtaining that values of q_0 are practically independents from bed height and different to experimental values. Mata et al. [45] predicted that Thomas model reproduces acceptably the breakthrough curves, obtaining experimental values of biosorption capacity very similar to calculated by the model.

Yoon and Nelson model. The Yoon and Nelson model is mathematically equivalent to Thomas model. From Eq. (10) and nonlinear regression, parameters model and adjusted values by model are obtained, they are shown in Table 5.

This model is not acceptable to reproduce the breakthrough curves (r^2 values less than 0.90). However, the values of time necessary to removal the 50% of initial metal, τ, are very nearly to obtain experimentally. These results coincide with obtained by other author studying different system biosorbent metal in a packed bed column [46,47].

Dose–response model. From Eq. (11) and nonlinear regression, parameters model and adjusted values are obtained. They are shown in Table 5.

The predicted breakthrough curves of the dose–response model show reasonably good agreement with the experimental plots ($r^2 > 0.90$). However, the values of the maximum concentration of the solute in the solid phase, q_0, are not agreed with experimental results.

However, the values of total amount of copper retain, q_{total}, obtained experimentally and obtained by adjust of the model are practically same (Table 6). As indicated above, this model reproduces acceptably the complete breakthrough curves, but, in some cases, it is difficult to relate adjusted parameters with operational conditions. Therefore, dose–response model is unusual for modeling the operation in the column and to perform a scaling of the process.

4. Conclusions

The present study shows that almond shell can be used as biosorbent for the removal of copper from aqueous solutions. Optimum biosorption conditions were determined by using a FFD. The model equation obtained led to a classification of the parameters based on their level of significance for two response analyzed (biosorption capacity and total copper removal). The optimization process concluded that the most influent parameters in biosorption capacity was initial concentration of Cu(II), while the most influential factors in total copper removal were the flow rate and mass of almond shell. The scatter graph of the predicted response values vs. experimental response values for total Cu(II) removal (% *R*) onto almond shell were studied, showing that experimental data are in good accordance with obtained through model. Adams–Bohart, Thomas, Yoon–Nelson, and dose–response models were used to fit the experimental data. Results shown that dose–response model was the best model to adjust the complete breakthrough curves.

Acknowledgements

The authors are grateful to the Spanish Ministry of Science and Innovation for financial support received (Project CTM2009-10294).

References

[1] B. Volesky, Z.R. Holan, Biosorption of heavy–metals, Biotechnol. Progr. 11 (1995) 235–250.
[2] S.P.K. Sternberg, R.W. Dorn, Cadmium removal using *Cladophora* in batch, semi-batch and flow reactors, Bioresour. Technol. 81 (2002) 249–255.
[3] A. Kapoor, T. Viraraghavan, Biosorption of heavy metals on *Aspergillus niger*: Effect of pretreatment, Bioresour. Technol. 63 (1998) 109–113.
[4] N. Ahalya, T.V. Ramachandra, R.D. Kanamadi, Biosorption of heavy metals, J. Chem. Environ. 7 (2003) 71–79.
[5] K.K. Singh, R. Rastogi, S.H. Hasan, Removal of Cr(VI) from wastewater using rice bran, J. Colloid Interface Sci. 290 (2005) 61–68.
[6] B. Volesky, Detoxification of metal-bearing effluents: Biosorption for the next century, Hydrometallurgy 59 (2001) 203–216.
[7] B. Benguella, H. Benaissa, Cadmium removal from aqueous solutions by chitin: Kinetic and equilibrium studies, Water Res. 36 (2002) 2463–2474.
[8] B.N. Estevinho, E. Ribeiro, A. Alves, L. Santos, A preliminary feasibility study for pentachlorophenol column sorption by almond shell residues, Chem. Eng. J. 136 (2008) 188–194.
[9] B. Hasan, O. Duygu, D. Celal, Biosorption of Rhodamine 6G from aqueous solutions onto almond Shell (*Prunus dulcis*) as a low cost biosorbent, Desalination 252 (2010) 81–87.
[10] F. Vegliò, F. Beolchini, M. Prisciandaro, Sorption of copper by olive mill residues, Water Res. 37 (2003) 4895–4903.
[11] Z.X. Xuan, Y.R. Tang, X.M. Li, Y.H. Liu, F. Luo, Study on the equilibrium, kinetics and isotherm of biosorption of lead ions onto pretreated chemically modified orange peel, Biochem. Eng. J. 31 (2006) 160–164.

[12] K.K. Krishnani, M.X. Xiaoguang, C. Christodoulatos, V.M. Boddu, Biosorption mechanism of nine different heavy metals onto biomatrix from rice husk, J. Hazard. Mater. 153(3) (2008) 1222–1234.
[13] M. Iqbal, A. Saeeda, A. Iqbal Zafar, FTIR spectrophotometry, kinetics and adsorption isotherms modeling, ion exchange, and EDX analysis for understanding the mechanism of Cd^{2+} and Pb^{2+} removal by mango peel waste, J. Hazard. Mater. 164 (2009) 161–171.
[14] M.E.R. Carmona, M.A.P. da Silva, S.G.F. Leite, Biosorption of chromium using factorial experimental design, Process Biochem. 40 (2005) 779–788.
[15] K. Ravikumar, S. Krishnan, S. Ramalingam, K. Balu, Application of response surface methodology to optimize the process variable for reactive Red and Acid Brown dye removal using a novel adsorbent, Dyes Pigm. 72 (2007) 66–74.
[16] Y. Safa, H. Nawaz, Kinetic and thermodynamic modeling for the removal of Direct Red-31 and Direct Orange-26 dyes from aqueous solutions by rice husk, Desalination 272 (2011) 313–322.
[17] C. Montgomery, Design and Analysis of Experiments, fifth ed., Wiley, New York, NY, 2001.
[18] S.H. Hasan, P. Srivastavaa, M. Talat, Biosorption of Pb(II) from water using biomass of *Aeromonas hydrophila*: Central composite design for optimization of process variables, J. Hazard. Mater. 168 (2009) 1155–1162.
[19] M. Calero, G. Blázquez, A. Ronda, M.A. Martín-Lara, Effect of the acid treatment of olive stone on the biosorption of lead in a packed-bed column, Ind. Eng. Chem. Res. 49 (2010) 12587–12595.
[20] G.E.P. Box, W.G. Hunter, J.S. Hunter, Statistics for Experimenters: An Introduction to Design, Data Analysis, and Model Building, Wiley, New York, NY, 1978.
[21] Z. Aksu, F. Gönen, Biosorption of phenol by immobilized activated sludge in a continuous packed bed: Prediction of breakthrough curves, Process Biochem. 39 (2004) 599–613.
[22] K. Vijayaraghavan, D. Prabu, Potential of *Sargassum wightii* biomass for copper(II) removal from aqueous solutions: Application of different mathematical models to batch and continuous biosorption data, J. Hazard. Mater. 137 (2006) 558–564.
[23] R. Han, D. Ding, Y. Xu, W. Zou, Y. Wang, Y. Li, L. Zou, Use of rice husk for the adsorption of Congo red from aqueous solution in column mode, Bioresour. Technol. 99 (2008) 2938–2946.
[24] B. Kiran, A. Kaushik, Cyanobacterial biosorption of Cr (VI): Application of two parameter and Bohart Adams models for batch and column studies, Chem. Eng. J. 144 (2008) 391–399.
[25] M. Calero, F. Hernáinz, G. Blázquez, G. Tenorio, M.A. Martín-Lara, Study of Cr(III) biosorption in a fixed-bed column, J. Hazard. Mater. 171 (2009) 886–893.
[26] G.S. Bohart, E.Q. Adams, Some aspects of the behaviour of the charcoal with respect chlorine, J. Am. Chem. Soc. 42 (1920) 523–544.
[27] H.C. Thomas, Heterogeneous ion exchange in a flowing system, J. Am. Chem. Soc. 66 (1944) 1664–1666.
[28] Y.H. Yoon, J.H. Nelson, Application of gas adsorption kinetics I. A theoretical model for respirator cartridge service life, Am. Ind. Hydrol. Assoc. J. 45 (1984) 509–516.
[29] G. Yan, T. Viraraghavan, Heavy metal removal in a biosorption column by immobilized *Mucor rouxii* biomass, Bioresour. Technol. 78 (2001) 243–249.
[30] R. Senthilkumar, K. Vijayaraghavan, M. Thilakavathi, P.V.R. Iyer, M. Velan, Seaweeds for the remediation of wastewaters contaminated with zinc(II) ions, J. Hazard. Mater. 136 (2006) 791–799.
[31] G.Y. Yan, T. Viraraghavan, M. Chen, A new model for heavy metal removal in a biosorption column, Adsorpt. Sci. Technol. 19 (2001) 25–43.
[32] M. Calero, F. Hernáinz, G. Blázquez, E. Dionisio, M.A. Martín-Lara, Evaluación de la biosorción de cobre con cáscara de almendra [Evaluation of copper biosorption by almond shell], Afinidad 554 (2011) 274–284.
[33] J.M. Brady, J.M. Tobin, J.-C. Roux, Continuous fixed bed biosorption of Cu^{2+} ions: Application of a simple two parameters mathematical model, J. Chem. Technol. Biotechnol. 74 (1999) 71–77.
[34] S. Baytak, A.R. Turker, The use of Agrobacterium tumefacients immobilized on Amberlite XAD–4 as a new biosorbent for the column preconcentration of iron (III), cobalt (II), manganese (II) and chromium (III), Talanta 64 (2005) 938–945.
[35] K. Vijayaraghavan, J. Jegan, K. Palanivelu, M. Velan, Biosorption of copper, cobalt and nickel by marine green alga *Ulva reticulate* in a packed column, Chemosphere 60 (2005) 419–426.
[36] Z. Zulfadhly, M.D. Mashitah, S. Bhatia, Heavy metals removal in fixed-bed column by the macro fungus *Pycnoporus sanguineus*, Environ. Pollut. 112 (2001) 463–470.
[37] K. Vijayaraghavan, J. Jegan, K. Palanivelu, M. Velan, Removal of nickel(II) ions from aqueous solution using crab shell particles in a packed bed upflow column, J. Hazard. Mater. 113 (2004) 223–230.
[38] H.M. Kim, J.G. Kim, J.D. Cho, J.W. Hong, Optimization and characterization of UV–curable adhesives for optical communication by response surface methodology, Polym. Test 22 (2003) 899–906.
[39] Y. Sag, Y. Aktay, Application of equilibrium and mass transfer models to dynamic removal of Cr(VI) ions by chitin in packed column reactor, Process Biochem. 36 (2001) 1187–1197.
[40] X. Liao, M. Zhang, B. Shi, Collagen-fiber-immobilized tannins and their adsorption of Au(III), Ind. Eng. Chem. Res. 43 (2004) 2222–2227.
[41] K. Pakshirajan, T. Swaminathan, Biosorption of copper and cadmium in packed bed columns with live immobilized fungal biomass of *Phanerochaete chrysosporium*, Appl. Biochem. Biotechnol. 157 (2009) 159–173.
[42] R. Han, L. Zou, X. Zhao, Y. Xu, F. Xu, Y. Li, Y. Wang, Characterization and properties of iron oxide-coated zeolite as adsorbent for removal of copper(II) from solution in fixed bed column, Chem. Eng. J. 149 (2009) 123–131.
[43] P. Saha, S. Datta, S.K. Sanyal, Application of natural clayey soil as adsorbent for the removal of copper from wastewater, J. Environ. Eng.—ASCE 136 (2010) 1409–1417.
[44] G. Vázquez, M. Sonia Freire, J. Gonzalez-Alvarez, G. Antorrena, Equilibrium and kinetic modeling of the adsorption of Cd^{2+} ions onto chestnut shell, Desalination 249 (2009) 855–860.
[45] Y.N. Mata, M.L. Blázquez, A. Ballester, F. González, J.A. Muñoz, Optimization of the continuous biosorption of copper with sugar-beet, J. Environ. Manage. 90 (2009) 1737–1743.
[46] G.A.R. Oliveira, E.R.A. Ferraz, F.M.D. Chequer, M.D. Grando, J.P.F. Angeli, M.S. Tsuboy, J.C. Marcarini, M.S. Mantovani, M.E. Osugi, T.M. Lizier, M.V.B. Zanoni, D.P. Oliveira, Chlorination treatment of aqueous samples reduces, but does not eliminate, the mutagenic effect of the azo dyes Disperse Red 1, Disperse Red 13 and Disperse Orange 1, Mutat. Res. 703 (2010) 200–208.
[47] G.M. Mulgund, S.P. Dabeer, S. Dhar, V. Makani, B. Jadhav, Equilibrium uptake and column studies of Pb^{+2}, Cu^{+2} and Cd^{+2}, using waste eucalytus charcoal, Aust. J. Basic Appl. Sci. 5 (2011) 135–142.